The American Journal of Human Genetics, Volume *99*

Supplemental Data

Mutations in Citron Kinase Cause Recessive Microlissencephaly with Multinucleated Neurons

Brian N. Harding, Amanda Moccia, Séverine Drunat, Omar Soukarieh, Hélène Tubeuf, Lyn S. Chitty, Alain Verloes, Pierre Gressens, Vincent El Ghouzzi, Sylvie Joriot, Ferdinando Di Cunto, Alexandra Martins, Sandrine Passemard, and Stephanie L. Bielas

Supplemental Data

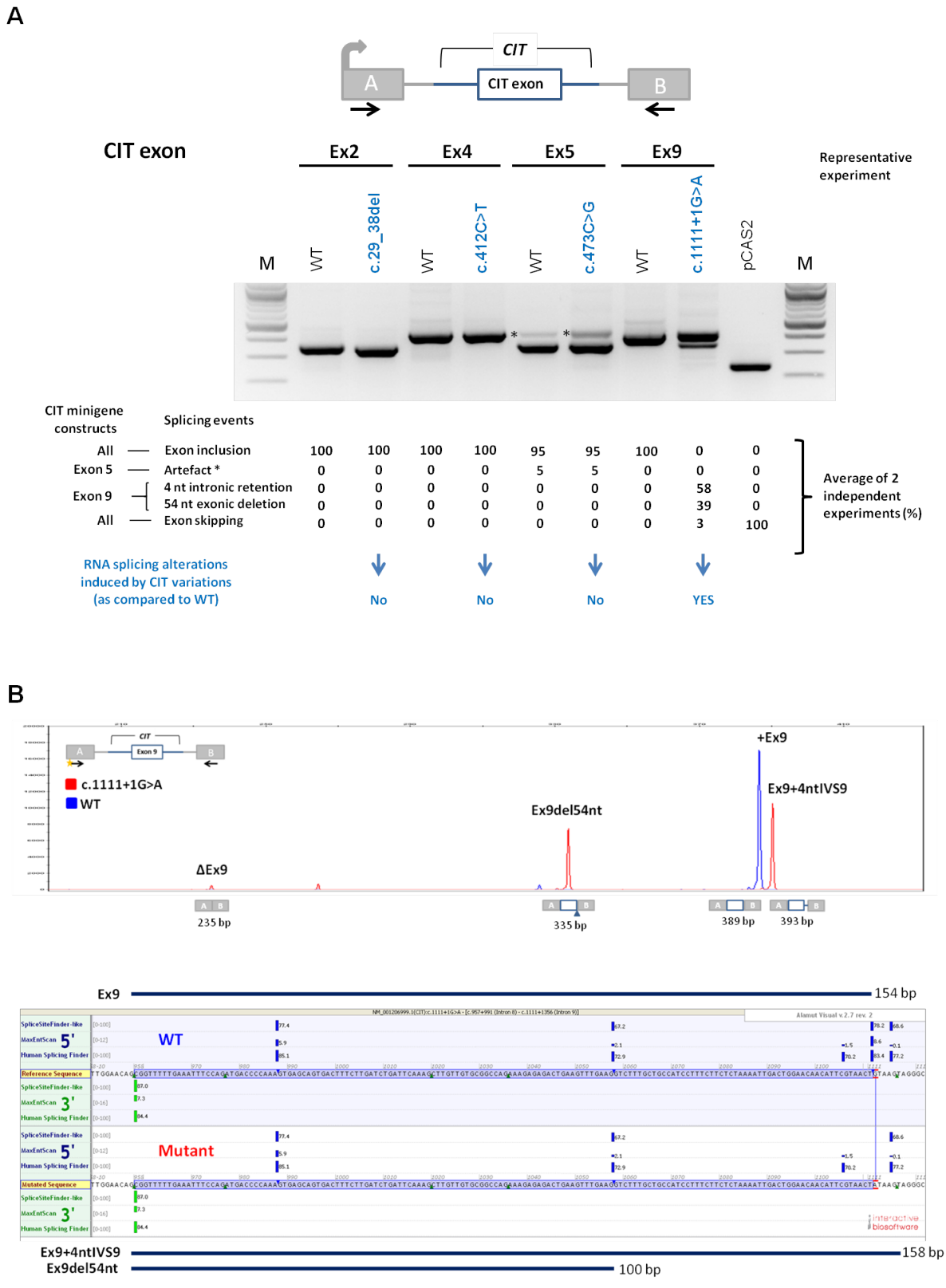

Figure S1. Detection of variant-induced *CIT* splicing alterations by using a minigene splicing assay. (A) Analysis of the splicing pattern of pCAS2 minigenes carrying *CIT* variants identified in microcephaly probands described in this study, as indicated. The top panel

represents the structure of pCAS2-CIT minigenes used in the minigene splicing assay. The grey arrow indicates the CMV promoter, boxes represent exons, lines in between indicate introns, and arrows below the exons represent primers used in RT-PCR reactions (Table S1). The minigenes were generated by inserting a genomic fragment containing the exon of interest and at least 150 nucleotides of the flanking introns into the intron of pCAS2, as described in Gaildrat et al. (either by using proband gDNA as template or by introducing the variants into the minigenes by site-directed mutagenesis)[1]. Then, wild-type (WT) and mutant constructs, as indicated, were transfected into HeLa cells and the minigenes' transcripts were analyzed by RT-PCR 24 hours later. The image shows the results of a representative experiment in which the RT-PCR products were separated on a 2.5% agarose gel stained with ethidium bromide and visualized by exposure to ultraviolet light. M indicates a 100 bp DNA ladder (New England Biolabs). The splicing events indicated under the gel are based on equivalent RT-PCR reactions performed by using a fluorescent forward primer (Table S1) and then separated in denaturing conditions by capillary electrophoresis on an automated sequencer (Applied Biosystems). Quantification results were obtained by using the GeneMapper v5.0 software (Applied Biosystems) and correspond to the average of two fluorescent-RT-PCR independent experiments. (B) Representative fluorescent RT-PCR experiment using pCAS2-*CIT* c.1111+1G>A-derived data as an example. The top panel shows superposed peaks corresponding to the WT and mutant products (in blue and red, respectively), as indicated. The bottom panel illustrates the outcome of the minigene assay relative to *CIT* exon 9 splicing both in the WT (top) and mutant (bottom) contexts, as well as *in silico* predictions relative to 5'ss and 3'ss in the genomic region of interest. *In silico* predictions were obtained by simultaneously interrogating 3 algorithms (SpliceSiteFinder-Like, MaxEntScan, and Human Splice Finder) through the integrated software tool Alamut (Interactive Biosoftware, France, http://www.interactive-biosoftware.com), as previously described[2]. For simplicity, thresholds for 5'ss and 3'ss scores were set at 66 and 84 for SpliceSiteFinder-Like, 0 and 7 for MaxEntScan, and at 70 and 84 for Human Splice Finder, respectively.

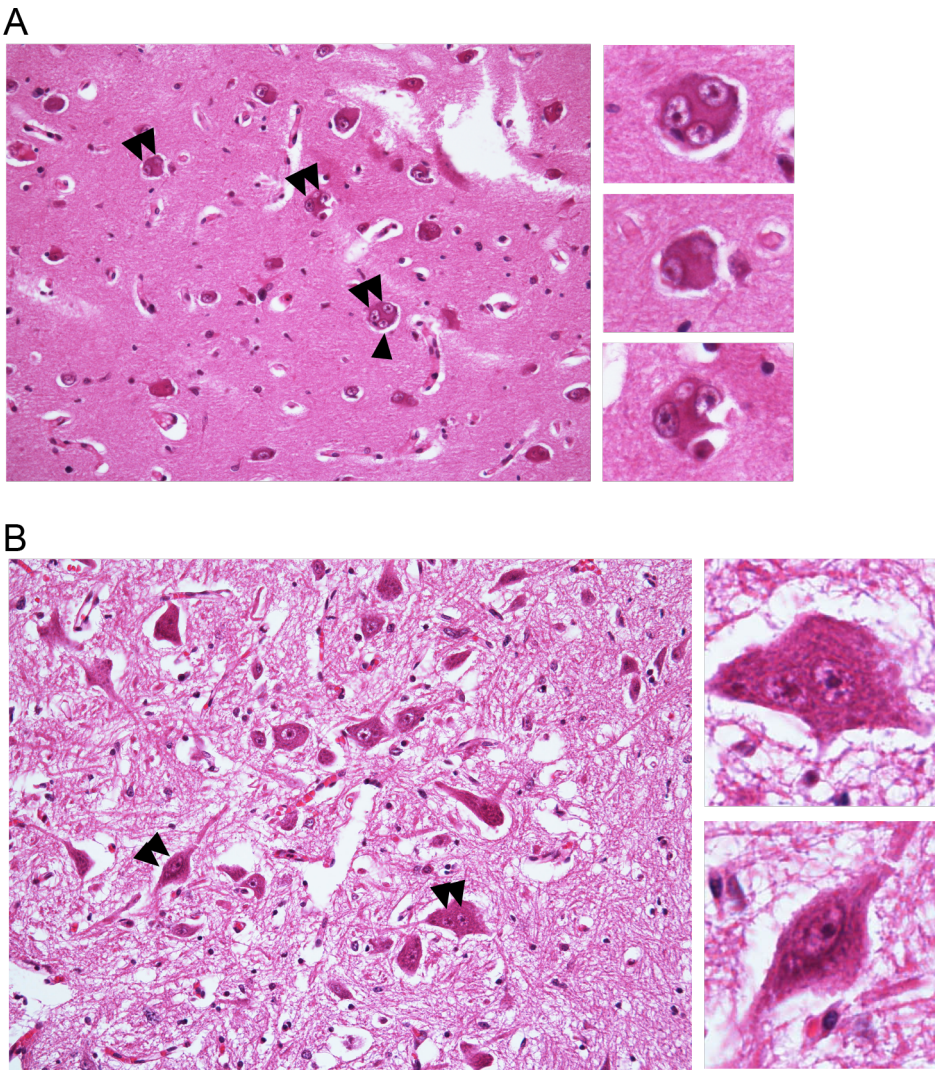

Figure S2. Multinucleated neurons throughout the neuraxis of Proband B. (**A**) Thalamus, (**B**) Spinal cord anterior horn. Cells indicated by arrowheads are enlarged in the inserts and multinucleated.

Table S1. Primers used in the pCAS2 minigene splicing assay for the analysis of *CIT* variations in exons 2, 4, 5 and 9.

Purpose	Forward (F) or reverse (R) primers	
	Name	Sequence (5'-3')
PCR (cloning/minigene preparation)	CIT_Ex2 InFus BamHI-F	AAGAAGTGCA*GGATCC*GTCAGATAAGTGTATCATCTCCTGTCA
	CIT_Ex2 InFus MluI-R	TCAAAACAAG*ACGCGT*TTCCCCTAAAATATTATCCCTGGTCC
	CIT_Ex4 InFus BamHI-F	AAGAAGTGCA*GGATCC*GTAGCTGCCATGGAAACTGTAC
	CIT_Ex4 InFus MluI-R	TCAAAACAAG*ACGCGT*CATCAAGAGGAATTTGTGAGCCTTC
	CIT_Ex5 InFus BamHI-F	AAGAAGTGCA*GGATCC*GGCTAAGTGACAGCCCCTTC
	CIT_Ex5 InFus MluI-R	TCAAAACAAG*ACGCGT*ACCACGTTCAGCCCAATGAG
	CIT.ex9.BamHI-F	TGGGAA*GGATCC*TTTGGTCCAAAGGGAAGAGGG
	CIT.ex9.MluI-R	ACTCAA*ACGCGT*CTACATCATTAGCCTTTACTACTCCTGTAG
Sequencing of minigene inserts	pCAS-Seq-F	GGGTCAATAGCAGTGAGAGG
	pCAS-Seq-R	GCTCCATTTCACAGGTAGAGA
Site-directed mutagenesis by two-stage overlap PCR	CIT Ex2 c.29_38del-F	ATATGGAGCGCGGA*TGCTGGTGCTGCTG*
	CIT Ex2 c.29_38del-R	CAGCAGCACCAGCA*TCCGCGCTCCATAT*
	CIT Ex4 c.412CT-F	GGCCCAGGAGTAGGTAGGAGG
	CIT Ex4 c.412CT-R	CCTCCTACCTACTCCTGGGCC
	CIT Ex5 c.473CG-F	GCCCGTGGATCCGCCAATTACAG
	CIT Ex5 c.473CG-R	CTGTAATTGGCGGATCCACGGGC
RT-PCR and sequencing of RT-PCR products	pCAS-KO1-F	TGACGTCGCCGCCCATCAC
	pCAS-2R	ATTGGTTGTTGAGTTGGTTGTC
Fluorescent RT-PCR	6FAM-pCAS-KO1-F	TGACGTCGCCGCCCATCAC
	pCAS-2R	ATTGGTTGTTGAGTTGGTTGTC

Table S2. Mammalian models of null mutations in *CIT.*

Species	**Human Proband B**	***Cit*$^{-/-}$ Knockout Mouse[3] (Di Cunto et al. 2000)**	***Flathead fh/fh* Mutant Rat[4,5] (Sarkisian et al. 2002) (Ackman et al. 2007)**
***Citron Kinase* Mutation**	10 bp deletion in exon 2	Conditional excision exon 2 by *Cre* mediated homologous recombination	Spontaneous 1 bp deletion in exon 1
Predicted Mutational Impact	Frameshift causing a premature stop codon 25 amino acids from start site	Premature stop codon	Frameshift causing a premature stop codon 27 amino acids from start site
***CIT* Transcript**	Predicted NMD	NMD	NMD
Brain Size and Weight	Microcephalic and ~1/10 of the brain weight of an average newborn	Microcephalic 50% brain weight reduction	Microcephalic 50% brain size reduction
Cerebral Cortex Abnormalities	Cortex shows cytological and organizational abnormalities. Six layer arrangement replaced by a molecular layer and two broad layers. Presence of multinucleated neurons.	40% reduction in cerebral cortex thickness. Disorganized lamination of 6-layer cortex. Presence of binucleated cells.	Neocortex displays a reduced number of neurons but normal lamination. Presence of binucleated neurons in neocortex.
Cerebellar Abnormalities	Hypoplastic and dysplastic cerebellar cortex, and disrupted laminar architecture. Crowded layer of Purkinje cells with simple dendritic arborizations. Binucleated Purkinje cells and granule cells.	70% cerebellum size reduction. Crowded layer of Purkinje cells with simple dendritic arborizations. Presence of binucleated cells.	Cerebellum displays a reduced number of neurons. Presence of binucleated neurons.
Hippocampal Abnormalities	Small and disorganized Ammon's horns. Only a small remnant of dentate fascia. Binucleated granule cells.	Normal Ammon's horn cell density and lamination. Essentially absent dentate gyrus.	Dentate gyrus displays a reduced number of neurons. Presence of binucleated neurons.
Additional Locations of Multinucleated Cells	Thalamus, striatum, pallidum, brain stem, spinal cord and PNS	Thalamus	Striatum, thalamus, midbrain, hindbrain, and spinal cord
Other Phenotypic Abnormalities	Kidney and heart defects, facial dysmorphisms, and rotated lower limbs	Ataxia, seizures, and failure to thrive	Seizures and disrupted development of the retina

NMD = Nonsense mediated decay, PNS = Peripheral Nervous System

Table S3. Presence of binucleated neurons by neuroanatomic area.

Presence of binucleated neurons by anatomic area	
neocortex	
hippocampus (pyramidal and granule cells)	
thalamus	
striatum (large and small cells)	
pallidum	
cerebellum	cerebellar cortex (Purkinje and granule cells)
	dentate nucleus
brain stem	midbrain tectum
	oculomotor nuclei
	pontine reticular formation
	nuclei pontis
	abducens nucleus
	inferior olive
	red nucleus
spinal cord & PNS	anterior horn
	autonomic ganglion

PNS = Peripheral nervous system

Supplemental References

1. Gaildrat, P., Killian, A., Martins, A., Tournier, I., Frébourg, T., and Tosi, M. (2010). Use of splicing reporter minigene assay to evaluate the effect on splicing of unclassified genetic variants. Methods Mol Biol 653, 249-257.

2. Soukarieh, O., Gaildrat, P., Hamieh, M., Drouet, A., Baert-Desurmont, S., Frébourg, T., Tosi, M., and Martins, A. (2016). Exonic Splicing Mutations Are More Prevalent than Currently Estimated and Can Be Predicted by Using In Silico Tools. PLoS Genet 12, e1005756.

3. Di Cunto, F., Imarisio, S., Hirsch, E., Broccoli, V., Bulfone, A., Migheli, A., Atzori, C., Turco, E., Triolo, R., Dotto, G.P., et al. (2000). Defective neurogenesis in citron kinase knockout mice by altered cytokinesis and massive apoptosis. Neuron 28, 115-127.

4. Sarkisian, M.R., Li, W., Di Cunto, F., D'Mello, S.R., and LoTurco, J.J. (2002). Citron-kinase, a protein essential to cytokinesis in neuronal progenitors, is deleted in the flathead mutant rat. J Neurosci 22, RC217.

5. Ackman, J.B., Ramos, R.L., Sarkisian, M.R., and Loturco, J.J. (2007). Citron kinase is required for postnatal neurogenesis in the hippocampus. Dev Neurosci 29, 113-123.